THESIS FOR THE DEGREE OF DOCTOR OF PHILOSOPHY

IN SOLID AND STRUCTURAL MECHANICS

# On the modelling of ultrasonic testing using boundary integral equation methods

Jonathan Westlund

Department of Applied Mechanics
Chalmers University of Technology
Gothenburg, Sweden 2011

On the modelling of ultrasonic testing using boundary integral equation methods
Jonathan Westlund
ISBN 978-91-7385-502-0



Doktorsavhandlingar vid Chalmers tekniska högskola
Ny serie nr 3183
ISSN 0346-718X

Department of Applied Mechanics
Chalmers University of Technology
SE-412 96 Gothenburg
Sweden
+46 (0)31-772 1000

Chalmers Reproservice
Gothenburg, Sweden 2011

On the modelling of ultrasonic testing using boundary integral equation methods

Jonathan Westlund
Department of Applied Mechanics
Chalmers University of Technology

# Abstract

Ultrasonic nondestructive testing has important applications in, for example, the nuclear power and aerospace industries, where it is used to inspect safety-critical parts for flaws. For safe and reliable testing, mathematical models of the ultrasonic measurement systems are invaluable tools. In this thesis such measurement models are developed for the ultrasonic testing for defects located near non-planar surfaces. The applications in mind are the testing of nuclear power plant components such as thick-walled pipes with diameter transitions, pipe connections, etc. The models use solution methods based on frequency domain boundary integral equation methods, with a focus on analytical approaches for the defects and regularized boundary element methods for the non-planar surfaces. A major benefit of the solution methods is the ability to provide accurate results both for low, intermediate and high frequencies. The solution methods are incorporated into a framework of transmitting probe models based on prescribing the traction underneath the probe and receiving probe models based on electromechanical reciprocity. Time traces are obtained by applying inverse temporal Fourier transforms, and it is also shown how calibration and effects of material damping can be included in the models.

Keywords: Elastic waves, Scattering, Nondestructive testing, Ultrasonics, Boundary integral equation method, Boundary element method, Regularization, $T$ matrix.

# Preface

This thesis reports the outcome of my research work as a PhD student at the Division of Dynamics during the period April 2006-January 2011. The research project has been sponsored by the Swedish Radiation Safety Authority, SSM, and this is gratefully acknowledged.

During the course of this work, several important contributions to the progress have been made. With sincere gratitude I wish to acknowledge these contributions: my supervisor, Prof. Anders Boström, has given excellent supervision, always made the time to discuss and show interest in my work, and has carefully read and given valuable feedback on all of my manuscripts; Dr. Per-Åke Jansson, my assistant supervisor, has also always made the time to discuss my work, and has also helped me with several computer related issues as well as calibration computations; Prof. Andrés Saéz, Universidad de Sevilla, made arrangements such that I could spend a rewarding month at the university of Seville in an active environment of prominent boundary element research; the Swedish National Committee for Theoretical and Applied Mechanics, SNM, provided financial support for the stay in Seville through the Folke Odqvist scholarship. For having created a nice environment to work in I also want to thank my colleagues, former and present, at the Division of Dynamics and the Division of Material and Computational Mechanics. I would finally like to express my deepest gratitude to my wife Jessica, for all the support and encouragement. I am a man of very good fortune.

Gothenburg, February 2011
Jonathan Westlund

# Thesis

This thesis consists of an extended summary and the following appended papers:

**Paper A**
J. Westlund.
2D SH modelling of ultrasonic testing for cracks near a non-planar surface.
Published in *Eng. Anal. Boundary Elem.*, 33:1103-1112, 2009.

**Paper B**
J. Westlund and A. Boström.
A 2D model of ultrasonic testing for cracks near a non-planar surface.
Published in *Wave Motion*, 47:383-394, 2010.

**Paper C**
J. Westlund.
Elastic wave scattering by a rectangular crack near a non-planar back surface.
Submitted for international publication, 2011.

**Paper D**
J. Westlund and A. Boström.
A hybrid $T$ matrix/boundary element method for elastic wave scattering from defects near a non-planar surface.
Submitted for international publication, 2011.

Two of the appended papers were prepared in collaboration with a co-author. The author of this thesis was responsible for the major progress of work in these papers, including developing the solution methods and numerical implementations, carrying out the numerical simulations and writing the main parts of the papers.

# Contents

**Abstract** **i**

**Preface** **iii**

**Thesis** **v**

## Extended Summary **1**

**1 Background and motivation** **1**

**2 Elastic wave propagation** **1**
2.1 Elastodynamics in 2D . . . . . 3

**3 Ultrasonic nondestructive testing** **3**
3.1 History of ultrasonic NDT . . . . . 5
3.2 Ultrasonic NDT methods . . . . . 6
3.3 Ultrasonic measurement models . . . . . 7

**4 Boundary integral equation methods** **9**
4.1 Singularities, regularization and numerical integration . . . . . 10
4.2 Truncation of infinite boundaries . . . . . 14

**5 Summaries of appended papers** **15**

**6 Concluding remarks and future work** **16**

**References** **17**

## Appended Papers **22**

# Extended Summary

The subject of this thesis is mathematical modelling of ultrasonic nondestructive testing (NDT) using boundary integral equation methods. The aim is to show how such methods can be used to develop measurement models for the ultrasonic testing for defects located near non-planar surfaces in, for example, nuclear power plant components.

The thesis is organized as follows. The background of and motivation for the work is given in section 1. In section 2 a brief account of the equations governing elastic wave propagation is given, followed by an introduction to ultrasonic NDT and measurement models for such testing in section 3. An overview of boundary integral equation methods for elastic wave propagation problems is given in section 4, and summaries of the appended papers are given in section 5. Concluding remarks and proposals for future work are offered in the final section of the extended summary, section 6, which is followed by the references and the appended papers A-D.

## 1 Background and motivation

Ultrasonic testing is currently the most commonly used method of nondestructive testing and evaluation, with especially important applications within the aerospace and nuclear power industries. For safe and reliable testing, a mathematical model of the ultrasonic measurement system is an invaluable tool. As a result, several ultrasonic measurement models have been developed. In most cases, however, these models are either based on approximate solution methods only valid for high frequencies/large defects, or based on methods requiring simple geometries with planar surfaces. In applications, on the other hand, many components such as nuclear power plant pipes with diameter transitions, bent pipes, pipe connections, etc., feature non-planar surfaces. The ultrasonic testing of such components is complicated by the fact that the signal response from a defect located close to a non-planar surface may be strongly influenced, or even completely masked, by the signal response from the non-planar surface. This makes the modelling of such testing situations especially important, and the models should preferably be based on solution methods capable of providing accurate results both for low, intermediate and high frequencies.

## 2 Elastic wave propagation

In ultrasonic NDT the amplitudes of the elastic waves are very small, typically of the order $1 - 10\,\mathrm{nm}$, and non-linear effects are normally negligible. For the applications in mind in this thesis; the ultrasonic testing of steel components such as pipes, the material can further

be assumed to be homogeneous and isotropic. The focus in this thesis is thus restricted to elastic wave propagation in linearly elastic, homogeneous and isotropic media. This section briefly reviews the equations governing elastic wave propagation in such media. For detailed expositions the reader is referred to any of the many books on the subject, e.g. Refs. [1, 9, 57].

The wave propagation in an elastic solid is governed by Cauchy's equation of motion:

$$\nabla \cdot \boldsymbol{\sigma} + \boldsymbol{b} = \rho \ddot{\boldsymbol{u}}, \tag{2.1}$$

where $\boldsymbol{\sigma}$ is the Cauchy stress tensor, $\boldsymbol{b}$ the body force, $\rho$ the mass density, $\ddot{\boldsymbol{u}}(\boldsymbol{x}, t) = \partial^2 \boldsymbol{u}/\partial t^2(\boldsymbol{x}, t)$ and $\boldsymbol{u}$ the displacement. For linearly elastic materials the Cauchy stress tensor $\boldsymbol{\sigma}$ is related to the elastic stiffness tensor $\boldsymbol{\mathcal{C}}$ and the strain $\boldsymbol{\varepsilon}$ by the linear stress-strain relation given by Hooke's law:

$$\boldsymbol{\sigma} = \boldsymbol{\mathcal{C}} : \boldsymbol{\varepsilon}.$$

Upon using the usual small-strain tensor:

$$\boldsymbol{\varepsilon} = \frac{1}{2}(\nabla \boldsymbol{u} + \boldsymbol{u} \nabla),$$

and the symmetry properties of $\boldsymbol{\mathcal{C}}$, Hooke's law may be rewritten as:

$$\boldsymbol{\sigma} = \boldsymbol{\mathcal{C}} : \nabla \boldsymbol{u}. \tag{2.2}$$

Only two elastic stiffness constants are required to characterize the behaviour of an isotropic material, and in elastodynamics the Lamé constants $\lambda$ and $\mu$ are normally used. For an isotropic and homogeneous material the elastic stiffness tensor may be expressed in terms of these constants as:

$$\boldsymbol{\mathcal{C}} = \lambda \mathbf{I}_2 \otimes \mathbf{I}_2 + 2\mu \mathbf{S}_4, \tag{2.3}$$

where $\mathbf{I}_2$ is the second-order identity tensor and $\mathbf{S}_4$ the symmetric fourth-order identity tensor. In the absence of body forces the combination of Hooke's law (2.2) and the elastic stiffness tensor given by Eq. (2.3) in Cauchy's equation of motion (2.1) yields the elastodynamic wave equation:

$$(\lambda + \mu) \nabla (\nabla \cdot \boldsymbol{u}) + \mu \nabla^2 \boldsymbol{u} = \rho \ddot{\boldsymbol{u}}.$$

This equation is also commonly denoted Navier's equation. By the use of the identity $\nabla^2 \boldsymbol{u} = \nabla(\nabla \cdot \boldsymbol{u}) - \nabla \times (\nabla \times \boldsymbol{u})$ the elastodynamic wave equation can be rewritten on the useful form:

$$(\lambda + 2\mu) \nabla (\nabla \cdot \boldsymbol{u}) - \mu \nabla \times (\nabla \times \boldsymbol{u}) = \rho \ddot{\boldsymbol{u}}. \tag{2.4}$$

It can be shown [1] that the displacement field $\boldsymbol{u}$ can be decomposed in displacement potentials $\varphi$ and $\boldsymbol{\psi}$ as $\boldsymbol{u} = \nabla\varphi + \nabla \times \boldsymbol{\psi}$, where the potential $\boldsymbol{\psi}$ satisfies the additional condition $\nabla \cdot \boldsymbol{\psi} = 0$. With this decomposition the displacement $\boldsymbol{u}$ is seen to consist of two wave motions: irrotational wave motion with propagation speed $((\lambda + 2\mu)/\rho)^{1/2}$ and divergence-free wave motion with propagation speed $(\mu/\rho)^{1/2}$. These motions are generally denoted P (primary, pressure) and S (secondary, shear) motions, and the corresponding wave speeds denoted $c_\mathrm{p}$ and $c_\mathrm{s}$, respectively.

For time-harmonic conditions with angular frequency $\omega$, such that $\boldsymbol{u}(\boldsymbol{x}, t) = \mathrm{Re}\,\{\boldsymbol{u}(\boldsymbol{x})\mathrm{e}^{-\mathrm{i}\omega t}\}$, it follows that $\ddot{\boldsymbol{u}} = -\omega^2\boldsymbol{u}$ so the elastodynamic wave equation (2.4) becomes:

$$k_\mathrm{p}^{-2}\nabla(\nabla \cdot \boldsymbol{u}) - k_\mathrm{s}^{-2}\nabla \times (\nabla \times \boldsymbol{u}) + \boldsymbol{u} = \boldsymbol{0}, \tag{2.5}$$

where $k_\mathrm{p} = \omega/c_\mathrm{p}$ is the pressure wave number and $k_\mathrm{s} = \omega/c_\mathrm{s}$ the shear wave number.

## 2.1 Elastodynamics in 2D

In 2D problems the displacement is independent of one coordinate, e.g. $x_3$. Then $\partial/\partial x_3 \equiv 0$ and the elastodynamic wave equation (2.5) decouples into two separate equations: one for the anti-plane displacement and one for the in-plane displacement. For the anti-plane displacement $\boldsymbol{u} = \boldsymbol{u}(x_1, x_2) = u_3(x_1, x_2)\mathbf{e_3}$, Eq. (2.5) immediately gives:

$$k_\mathrm{s}^{-2}\nabla^2 u_3(x_1, x_2) + u_3(x_1, x_2) = 0. \tag{2.6}$$

The time-harmonic anti-plane wave motion is thus governed by Helmholtz equation. This wave motion is usually called horizontally polarized shear motion, or SH in short.

For the in-plane motion two cases can be considered: plane stress and plane strain. The plane stress case, with $\sigma_{13} = \sigma_{23} = \sigma_{33} = 0$, is a relevant approximation for the in-plane motion of, for example, thin plates. For the models developed in this thesis, however, the applications in mind are ultrasonic testing of components such as thick-walled pipes, and for these applications only the plane strain case is relevant. In that case the anti-plane displacement vanishes identically so $\boldsymbol{u} = \boldsymbol{u}(x_1, x_2) = u_1(x_1, x_2)\mathbf{e_1} + u_2(x_1, x_2)\mathbf{e_2}$. This wave motion, which is a coupled motion of compressional and vertically polarized shear motion, is commonly abbreviated P-SV. The governing equation for this motion is given by Eq. (2.5), with $\boldsymbol{u}$ a vector field independent of $x_3$ and with only two components. In contrast, the elastic wave motion in 3D is in general a superposition of P, SV and SH motions which are coupled.

# 3 Ultrasonic nondestructive testing

A nondestructive testing (NDT) method is a method to "examine an object, material or system without impairing its future usefulness" [8]. A typical objective of such an

examination is the detection of defects such as cracks, voids, inclusions, corrosion, etc. The term nondestructive evaluation (NDE) is used to denote nondestructive testing methods where the results of the testing are used to evaluate the test object, and this normally entails a more quantitatively oriented testing and interpretation of the test results. As an example, a defect detection in a component may be followed by additional testing to determine size, shape and orientation of the defect in order to subsequently evaluate the structural integrity of the component. To further accentuate these differences the term quantitative nondestructive evaluation (QNDE) is also often used.

Several NDT methods exist today, of which the most common are [13]: radiology (X-ray methods), electrical and magnetic methods (eddy current testing, magnetic particle inspection, etc.), visual inspection, liquid penetrant testing and ultrasonic testing. Of these methods ultrasonic testing is currently the most widely used. Common applications include materials characterization studies and manufacturing process monitoring and control. The perhaps most important areas of application, however, are within the nuclear power and aerospace industries where ultrasonic NDT is used to inspect components for flaws during in-service use. Ultrasonic NDT plays a very important role in ensuring safe and reliable performance in these industries, where failure of a safety-critical component can have catastrophic consequences.

Some of the major advantages of ultrasonic NDT methods, which have promoted their widespread use, are:

- the ability to perform testing with only single-sided access to the component,
- superior penetration depth compared to other NDT methods,
- minimal interference with operations,
- fast response permitting rapid and automated testing,
- good accuracy of defect detection and characterization.

Principle drawbacks are the extensive needs of training and experience of the operator, and that the requirements on a high and constant degree of coupling between the probe and the scanning surface can be difficult to meet.

All ultrasonic NDT methods are based on emitting high-frequency acoustic or elastic waves into the test specimen. The term ultrasound denotes sound of frequencies above 20 kHz, which is approximately the upper limit of the audible range of a human ear. Also audible sound can be used for defect detection purposes; a familiar example is to check pots and chinaware for cracks by listening for changed ringing notes when tapping it. In most technical applications, however, the higher frequency ultrasound is used instead of audible sound. The main reasons are that the higher frequency (and thus shorter wavelength) enables detection of smaller defects, and since higher frequencies permit wave pulses of shorter duration the axial resolution improves. Also the lateral resolution improves, since the directivity of ultrasonic beams increase with frequency. On the other hand the attenu-

ation also increases with increasing frequency such that penetration depth is reduced, and this sets an upper limit to the range of useful frequencies for testing of a specific material. The attenuation is a combined effect of absorption and scattering, but for materials such as steel the scattering from the grain boundaries is the dominating attenuation effect setting the upper frequency limit. In all ultrasonic testing a compromise between resolution and penetration depth must thus be made, such that in the technical applications considered in this thesis the frequency of the employed ultrasound is typically in the range $0.1 - 10\,\mathrm{MHz}$.

## 3.1 History of ultrasonic NDT

An obvious prerequisite for all ultrasonic NDT methods is a means of generating the ultrasound. The history of ultrasound thus started in 1847 with Joule's discovery of magnetostriction. Even more important was the discovery by the Curie brothers in 1880 of the piezoelectric effect, which is presently the most widely used electroacoustic transduction mechanism for ultrasonic wave generation and detection. The first use of ultrasound for NDT purposes was proposed by Sokolov in 1929, in a method based on continuous wave through-transmission. In this set-up a continuous ultrasonic wave is transmitted from one side of the specimen and an ultrasonic receiver is placed on the other. Shadow areas indicating flaws in the specimen are then sought for. Major drawbacks of the method are that access to both sides of the specimen is required, the sensitivity is low and defect distance measurements are not possible. The introduction of ultrasonic pulse reflection testing, independently invented in the early 1940s by Firestone in America and by Sproule in England, was a milestone in the development of ultrasonic NDT as it made high accuracy, single-sided access testing with defect localization possible. Firestone received a patent for his "Supersonic Reflectoscope" in 1949, a pulse-echo testing[1] instrument incorporating a piezoelectric crystal to generate a short ultrasonic wave pulse which is transmitted in a narrow beam through the test specimen. Defects in the specimen then reflect ultrasonic energy back to the piezo crystal, which now acts as a microphone registering the pulses and travel times. These are then displayed on an oscilloscope for interpretation by an operator. The principles of this testing method have been virtually unchanged since then, and by 1955 pulse-echo testing was the dominant ultrasonic NDT method and it still remains the most important.

For detailed surveys of the historical development of ultrasonics the reader is referred to the book by Krautkrämer and Krautkrämer [40] and the Nondestructive Testing Handbook [44].

[1] The term pulse-echo testing is often used to denote pulse reflection testing using a single probe as both transmitter and receiver, as in Firestone's reflectoscope. Sproule's invention, on the other hand, featured two separate probes and the term pulse-echo is sometimes used also for this testing set-up. In this thesis, however, pulse-echo testing is solely used to denote those single-sided pulsed wave testing set-ups which use the same probe as both transmitter and receiver.

## 3.2 Ultrasonic NDT methods

Ultrasonic NDT methods can be divided into two types: contact testing and non-contact testing. In contact testing the ultrasonic probes are in touch with the test object surface. However, if the probe is applied directly to the surface of the test object most of the ultrasonic energy is reflected back again. The reflection is caused by the great mismatch in acoustic impedance of the solid material (of the test object) and the thin air gap (between the probe and test object surfaces). For this reason a couplant in the form of a liquid, grease or paste is usually applied to increase the transmission of ultrasonic energy into the test object. With the use of an appropriate couplant, contact testing generally has a high level of energy transfer. Other advantages of contact methods are high accessibility and small interference with operations, such that testing during in-service use of the component is often possible. An example of a non-contact testing method is immersion testing, where the probe(s) and the component are immersed in a water bath. Immersion testing has the benefit of providing a constant coupling to the component, which may be difficult to attain in contact testing when the probe is moved in a scan. Non-contact testing can also be performed using electromagnetic acoustic transducers (EMATs). These are based on inducing a magnetic field and a current in the component, which by the Lorentz force interact to generate mechanical waves in the component. Another more recently developed non-contact method is laser generated ultrasound. The latter two techniques are especially useful for moving measurement set-ups and testing of very hot components, but compared to standard contact testing using piezoelectric probes the efficiency of EMATs is very low and the laser equipment bulky and expensive.

The most commonly used ultrasonic probes, which are standard contact probes, consist of a piezoelectric crystal attached between two electrodes, a backing layer and a plastic wedge. The backing layer (the damping block) is applied to the electrode on the back face of the crystal, and acts as an attenuator controlling the shape and duration of the output pulse. The electrode on the front face of the crystal is applied to a plastic wedge which determines the wave type and angle of the beam transmitted into the component beneath the probe. The probe is normally characterized by the type of wave motion it generates inside the testing component: compressional (P-probe), horizontally polarized shear (SH-probe) or vertically polarized shear (SV-probe). In contact probes of the SH type the piezoelectric crystal generates shear motion inside the probe. For this motion to be transmitted to the testing component the couplant must be capable of transmitting shear motion. Glue, resin or some other highly viscous couplant must then be used. This renders the probe essentially immobile and scans are thus not possible. For this reason this kind of SH probe is not very often used in applications. Instead an EMAT, which is capable of generating SH waves in the solid while still allowing scans to be performed, is a good choice. P and angled SV contact probes, on the other hand, are normally based on piezoelectric crystals generating compressional motion inside the probes. Depending on the plastic wedges used, this motion is then refracted as a P, SV or combination of both wave types in the component. These probes are generally the preferred contact probe

choice, since they do not depend on the use of a viscous couplant capable of transmitting shear motion.

Surveys of ultrasonic techniques and applications are given in Refs. [13, 32, 40, 41, 44]. A detailed survey of different ultrasonic probes is given by Silk [55].

## 3.3 Ultrasonic measurement models

An ultrasonic nondestructive measurement system is not difficult to set up and employ: in the case of pulse-echo contact testing, a voltage is simply applied over a piezoelectric crystal. The resulting deformation is transmitted to the component, via a couplant, where it generates ultrasonic waves. The waves propagate in the component and are scattered by a defect. The ultrasound scattered back to the probe deforms the piezoelectric crystal, which then produces an output voltage. The difficulties instead arise when the results of the measurement - the input and output voltages - are to be interpreted quantitatively to determine, for example, defect size, shape and orientation. In order to provide this information based on the input and output voltages, a knowledge of the physics of the ultrasonic measurement process is required. One way of obtaining this knowledge is to pair the measurements with a detailed model of the entire ultrasonic measurement system - an ultrasonic measurement model. The purpose of such a model is to predict the measurement system's response due to specific flaws in the testing object.

There are major benefits of access to a measurement model: in addition to being invaluable in the interpretation of experimental data, it allows for parametric studies to be performed numerically such that costly and time-consuming experiments can be reduced to a minimum. This is useful both when designing and optimising testing procedures and equipment, and in the assessment of probability of detection of defects. Models are also valuable tools in the qualification of testing procedures and personnel.

An ultrasonic measurement model should include the generation of the incident ultrasound by the transmitting probe, the interaction of this wave field with different defects, and the generation of the output signal at the receiving probe due to excitation by the wave field scattered by the defect. In addition, different propagation characteristics such as effects of possible material anisotropy, attenuation, noise mechanisms, etc., should be accounted for. A complete model should also include calibration by standard defects such as side-drilled holes. The basis of all measurement models, however, is formed by the solution method used to solve the elastic wave propagation problem accounting for the interaction of the ultrasound with the defect. Since there are only very few cases where exact, closed form solutions exist, approximate numerical solution methods are generally the only possible alternatives. The challenge then lies in making approximations that lead to acceptable computation times, while retaining enough accuracy to provide useful results.

Several different strategies have been adopted in attempts to strike this balance. High-

frequency approximations such as elastodynamic Kirchoff theory [39] and elastodynamic Geometrical Theory of Diffraction (GTD) [5, 38] are commonly used, with examples such as the industry standard software CIVA [26, 27] and the model by Chapman [28]. Both these models use combinations of the Kirchhoff approximation and the GTD: the reflection of near-specular beams is computed using the Kirchhoff approximation, while the edge diffraction echoes from non-specular beams are computed using the GTD. Based on these approximations, powerful and computationally fast models can be developed. Complex geometries and defects, also in anistropic and inhomogeneous materials, can be treated. CIVA has also been favourably validated in several benchmark studies, see e.g. Refs. [48, 49]. Main drawbacks are the fact that the approximations are only valid for high frequencies/large defects, such that defect dimensions of at least a couple of wavelengths are typically required. Identifying the bounds of applicability more precisely in a specific case is also in general difficult, and in many cases the intermediate frequency range with defect dimensions comparable to the wavelength is also of great interest.

Alternatively, purely numerical methods like the finite difference method (FDM) or the finite element method (FEM) can be used. Examples of models based on finite difference methods, which in elastodynamics usually take the form of the elastodynamic finite integration technique (EFIT), are given by Fellinger [33] and Halkjær [35]. The EFIT has also been used more recently to model advanced guided wave testing applications [12, 36]. Examples of recent models based on the FEM are given by Refs. [42, 62]. Just like the high-frequency approximations, the EFIT and the FEM allow for very general geometries and materials. In addition, they can provide accurate results for all frequencies. In 3D, however, these volume discretization methods often generate excessively many nodes such that the computation times become restrictively long. The use of the FEM is thus still mainly restricted to 2D models, and there are also problems with grid dispersion and truncation errors [37, 50].

Another alternative is to use boundary integral equation methods (BIEMs), where the scattering problem is reformulated as a set of integral equations over the defect boundary and possibly also some other boundary. Just like the FEM and EFIT, BIEMs can provide accurate results for all frequencies. In addition, in BIEMs the unknowns are the field variables on the boundary only such that the problem dimensionality is reduced by one. This implies that for many wave propagation problems, BIEMs are computationally more efficient than volume discretization methods. Boundary integral equation methods are the focus of the present thesis, and are discussed further in section 4.

The value, practical use and construction of measurement models are discussed in the book by Schmerr [52], the papers by Achenbach [2–4] and the paper by Thompson and Gray [60]. Mathematical modelling of ultrasonic contact probes, an interesting research topic in its own right, is discussed in the books by Silk [55] and Schmerr [52], the paper by Boström

and Wirdelius [20] and in the PhD thesis by Wirdelius [64].

# 4 Boundary integral equation methods

The term boundary integral equation methods (BIEMs) denotes solution methods based on rewriting the governing equations as boundary integral equations, in terms of a Green's tensor and the field on the boundary, and subsequently solving the integral equations in some suitable fashion. The solution then yields the field variables on the boundary, and the field elsewhere can be computed using a corresponding integral representation. In wave propagation problems, BIEMs have the benefit of automatically incorporating the radiation condition in the solution. Other advantages are high accuracy and the reduction in problem dimensionality. However, since the reformulation is based on use of a Green's tensor, computing this tensor must have a low computational cost for the BIEM to be computationally efficient. This condition normally restricts the applicability of BIEMs to problems in homogeneous media with linear governing equations. For larger problems with many unknowns, isotropic or transversely isotropic [53] materials are also normally required. Another drawback of BIEMs, discussed in Refs. [14, 43, 65] and paper A, is that they can degenerate when applied to thin bodies such as cracks. This problem is circumvented by using a correct formulation of the boundary integral equations, which in the case of zero-width cracks is a hypersingular traction boundary integral equation.

The boundary element method (BEM) is a method to numerically solve boundary integral equations. The method consists of discretizing the boundary using boundary elements, which are line elements for 2D problems and surface elements for 3D problems. Linear algebraic equations for the field variables at the interpolation nodes of the boundary elements are then generated using point collocation or Galerkin's method. The representation of the boundary geometry and the interpolation of field variables on the boundary is usually performed with methods from finite element methods, for example isoparametrical interpolations with Lagrangian interpolation functions. For crack problems, however, interpolation functions incorporating the singular stress behaviour in the vicinity of the crack tips/edges are normally used, see e.g. Refs. [7, 45, 54, 65]. For cracks of complex shapes these discretizations can be difficult to implement, so even though the proposed discretizations are of more general validity the applications are normally restricted to simply shaped cracks.

As an alternative to the BEM, some simple crack geometries allow for an analytical approach based on expanding the unknown crack opening displacement in the hypersingular integral equation in a set of appropriate expansion functions. In combination with Galerkin's method to generate the equations for the expansion coefficients, this approach automatically resolves the difficulties associated with hypersingular integrals and results in a very computationally efficient numerical procedure. Crack geometries for which this approach is possible include strip-like cracks [25], rectangular cracks [16,19,34] and circular cracks [18]. In papers A-C this approach is adopted to treat the cracks, in a novel hybrid

solution method coupling this approach for the crack with an indirectly regularized (see section 4.1) displacement BEM for the back surface.

Another way of treating the scattering of elastic waves by defects is by the transition ($T$) matrix. The $T$ matrix gives the linear relationship between the expansion coefficients (in some suitable set of expansion functions) of the scattered waves and the incident waves. In several cases the $T$ matrix can be computed using efficient, analytically oriented approaches (see e.g. Refs. [15, 46, 63]), but the $T$ matrix of in principle any defect can otherwise be computed using numerical methods such as the FEM or the BEM. In paper D a novel boundary element method is developed using the $T$ matrix representation of a defect. In this method the defect is incorporated into the BEM for the back surface by using the Green's tensor for the defect, which is expressed using the $T$ matrix.

A survey of the history of BIEMs and the BEM is given by Cheng and Cheng [29]. Useful introductions to the BEM are provided by the books by Brebbia and co-authors [21–23]. The book by Bonnet [14] also serves as an excellent introduction, as well as containing more advanced topics. The book by Domínguez [31] is devoted to the BEM for dynamic problems. Advanced BIEMs for crack problems are discussed in the book by Zhang and Gross [65]. Although only treating statics, the book by Beer [10] is a very useful reference for general FORTRAN implementations of the BEM. A review of analytically oriented BIEMs for crack problems, and their applications in developing ultrasonic measurement models, is given by Boström [17]. The $T$ matrix method and related topics are discussed in Ref. [61].

## 4.1 Singularities, regularization and numerical integration

A characteristic feature of the boundary element method is the presence of singular element integrals, and the accurate computation of these singular integrals is a key ingredient of any implementation of the BEM. The singularities are introduced by the reformulation in terms of a Green's tensor, which by construction is singular. In this thesis the isotropic outgoing wave Green's tensor, here denoted $\boldsymbol{U}^k(\boldsymbol{x}, \boldsymbol{y}; \omega)$, is used. It is defined as the outward propagating solution of the equation:

$$\nabla \cdot \boldsymbol{\Sigma}^k(\boldsymbol{x}, \boldsymbol{y}; \omega) + \rho\omega^2 \boldsymbol{U}^k(\boldsymbol{x}, \boldsymbol{y}; \omega) = -\delta(\boldsymbol{x} - \boldsymbol{y})\mathbf{e}_k, \tag{4.1}$$

where the corresponding stress tensor is $\boldsymbol{\Sigma}^k(\boldsymbol{x}, \boldsymbol{y}; \omega) \equiv \boldsymbol{\mathcal{C}} : \nabla \boldsymbol{U}^k(\boldsymbol{x}, \boldsymbol{y}; \omega)$, $\delta(\boldsymbol{x} - \boldsymbol{y})$ denotes the 2D/3D Dirac delta distribution and $\mathbf{e}_k$ is the unit vector in the $k$-direction, $k = 1, 2$ or $k = 1, 2, 3$ in 2D or 3D, respectively. Letting $\{E_e\}_{e=1}^{N_e}$ denote the boundary elements, the singular element integrals occuring in the implementations of the BEM in this thesis are of the type:

$$\int_{E_e} u_i(\boldsymbol{x}) \Sigma_{ij}^k(\boldsymbol{x}, \boldsymbol{y}_{n_c}; \omega) \mathrm{n}_j(\boldsymbol{x}) \, \mathrm{d}S_{\boldsymbol{x}}, \tag{4.2}$$

where $\boldsymbol{u}$ is the displacement; $\boldsymbol{x}$, as indicated, the integration variable; $\boldsymbol{y}_{n_c}$ the collocation node which for singular element integrals is located on the integration element $E_e$; and $\mathbf{n}$ the unit normal vector.

The singular behaviour of $\Sigma_{ij}^k(\boldsymbol{x}, \boldsymbol{y}_{n_c}; \omega)$, as $r = |\boldsymbol{x} - \boldsymbol{y}_{n_c}| \to 0$, is $\Sigma_{ij}^k(\boldsymbol{x}, \boldsymbol{y}_{n_c}; \omega) = \mathcal{O}(r^{-1})$ in 2D and $\Sigma_{ij}^k(\boldsymbol{x}, \boldsymbol{y}_{n_c}; \omega) = \mathcal{O}(r^{-2})$ in 3D. Because of this singular behaviour, accurate computation of the integral (4.2) requires additional attention as compared to the element integrals occuring in finite element methods. A number of different methods have been proposed to achieve this, several of which are discussed in a book devoted to the subject [56]. In this thesis, however, an approach based on indirect regularization [14] is followed. In this approach terms are subtracted and added back in the integral equation, such that instead of the integral (4.2) one is led to consider the following element integrals:

$$u_i(\boldsymbol{y}_{n_c}) \int_{E_e} \Sigma_{ij}^k(\boldsymbol{x}, \boldsymbol{y}_{n_c}) \mathrm{n}_j(\boldsymbol{x}) \, \mathrm{d}S_{\boldsymbol{x}}, \tag{4.3a}$$

$$\int_{E_e} u_i(\boldsymbol{x}) \left[ \Sigma_{ij}^k(\boldsymbol{x}, \boldsymbol{y}_{n_c}; \omega) - \Sigma_{ij}^k(\boldsymbol{x}, \boldsymbol{y}_{n_c}) \right] \mathrm{n}_j(\boldsymbol{x}) \, \mathrm{d}S_{\boldsymbol{x}}, \tag{4.3b}$$

$$\int_{E_e} [u_i(\boldsymbol{x}) - u_i(\boldsymbol{y}_{n_c})] \Sigma_{ij}^k(\boldsymbol{x}, \boldsymbol{y}_{n_c}) \mathrm{n}_j(\boldsymbol{x}) \, \mathrm{d}S_{\boldsymbol{x}}, \tag{4.3c}$$

where $\Sigma_{ij}^k(\boldsymbol{x}, \boldsymbol{y}_{n_c})$ is the static Green's tensor: the solution to Eq. (4.1) for $\omega = 0$. Since the integrand of integral (4.3a) is simply the static Green's tensor, the integral can be evaluated analytically by an appropriate application of the divergence theorem. In addition, since the singular behaviour of $\Sigma_{ij}^k(\boldsymbol{x}, \boldsymbol{y}_{n_c}; \omega)$ and $\Sigma_{ij}^k(\boldsymbol{x}, \boldsymbol{y}_{n_c})$ is the same the difference is nonsingular such that numerical computation of (4.3b) is straightforward. Finally, if $\boldsymbol{u}$ is Hölder continuous; $|\boldsymbol{u}(\boldsymbol{x}) - \boldsymbol{u}(\boldsymbol{y}_{n_c})| \leq C|\boldsymbol{x} - \boldsymbol{y}_{n_c}|^\alpha$ for some $C > 0$ and $\alpha \in (0, 1]$, then the integral (4.3c) is at the worst weakly singular. In fact, with the interpolation used in this thesis also this integral becomes nonsingular and can be transformed to regular integrals which can be computed using ordinary Gauss quadrature. This is discussed in the following for the 3D case with the 9-noded quadrilateral isoparametric element used in paper C and depicted in Fig. 4.1, but the result may readily be specialized to the corresponding 2D case for which it remains true. The 2D case is considerably simpler since the boundary elements are then just line elements, and no element subdivision is necessary.

Introduce the global node number $m(e, q)$ for the local node $q \in \{1, 2, \ldots, 9\}$ on the physical element $E_e$, $e \in \{1, 2, \ldots, N_e\}$, and let $\boldsymbol{\xi} = (\xi_1, \xi_2) \in [-1, 1] \times [-1, 1]$ be the local coordinates in the parent element as depicted in Fig. 4.1. The coordinates of the node $m(e, q)$ are then denoted $\boldsymbol{x}^{m(e,q)}$ and the displacement of the same node is denoted $\boldsymbol{u}^{m(e,q)}$. In the isoparametrical interpolation with biquadratic Lagrangian interpolation functions

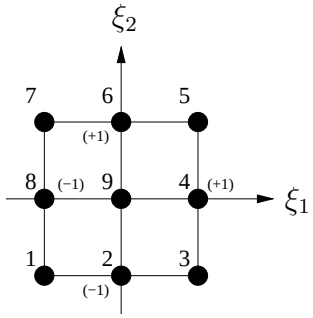


**Figure 4.1:** The parent element of a nine-noded quadrilateral boundary element.

$\{\phi_q\}_{q=1}^9$, the elementwise representations on element $E_e$ can be written:

$$\begin{cases} \boldsymbol{x} = \boldsymbol{x}^e(\boldsymbol{\xi}) = \sum_{q=1}^{9} \phi_q(\boldsymbol{\xi}) \boldsymbol{x}^{m(e,q)}, \\ \boldsymbol{u}(\boldsymbol{x}) = \boldsymbol{u}^e(\boldsymbol{x}^e(\boldsymbol{\xi})) = \sum_{q=1}^{9} \phi_q(\boldsymbol{\xi}) \boldsymbol{u}^{m(e,q)}, \\ \mathbf{n}(\boldsymbol{x}) = \mathbf{n}^e(\boldsymbol{x}^e(\boldsymbol{\xi})) = \boldsymbol{a}_{\mathbf{1}}^e(\boldsymbol{\xi}) \times \boldsymbol{a}_{\mathbf{2}}^e(\boldsymbol{\xi}) / |\boldsymbol{a}_{\mathbf{1}}^e(\boldsymbol{\xi}) \times \boldsymbol{a}_{\mathbf{2}}^e(\boldsymbol{\xi})|, \\ \mathrm{d}S_{\boldsymbol{x}} = |\boldsymbol{a}_{\mathbf{1}}^e(\boldsymbol{\xi}) \times \boldsymbol{a}_{\mathbf{2}}^e(\boldsymbol{\xi})| \, \mathrm{d}\xi_1 \mathrm{d}\xi_2, \end{cases}$$

where $\boldsymbol{a}_{\boldsymbol{j}}^e(\boldsymbol{\xi})$, $j$=1,2, are the tangent vectors of the physical element. Let $\boldsymbol{\eta}$ be the local coordinates in the parent element of the collocation point, such that:

$$\boldsymbol{y}_{n_c} = \boldsymbol{x}^e(\boldsymbol{\eta}) = \sum_{q=1}^{9} \phi_q(\boldsymbol{\eta}) \boldsymbol{x}^{m(e,q)}.$$

By Taylor's formula it follows that there exist modified interpolation functions $\hat{\phi}_q(\rho, \alpha; \boldsymbol{\eta})$ such that the difference $\phi_q(\boldsymbol{\xi}) - \phi_q(\boldsymbol{\eta})$ can be rewritten as:

$$\phi_q(\boldsymbol{\xi}) - \phi_q(\boldsymbol{\eta}) = \rho \hat{\phi}_q(\rho, \alpha; \boldsymbol{\eta}),$$

in terms of the polar coordinates $(\rho, \alpha)$ of the parent element with origin at the collocation point: $\boldsymbol{\xi} = \boldsymbol{\eta} + \rho(\cos\alpha, \sin\alpha)$. Using the modified interpolation functions, the first factor of the integrand of integral (4.3c) can be rewritten as:

$$\boldsymbol{u}(\boldsymbol{x}) - \boldsymbol{u}(\boldsymbol{y}_{n_c}) = \boldsymbol{u}^e(\boldsymbol{x}^e(\boldsymbol{\xi})) - \boldsymbol{u}^e(\boldsymbol{x}^e(\boldsymbol{\eta})) = \sum_{q=1}^{9} \left[\phi_q(\boldsymbol{\xi}) - \phi_q(\boldsymbol{\eta})\right] \boldsymbol{u}^{m(e,q)}$$

$$= \sum_{q=1}^{9} \rho \hat{\phi}_q(\rho, \alpha; \boldsymbol{\eta}) \boldsymbol{u}^{m(e,q)}.$$

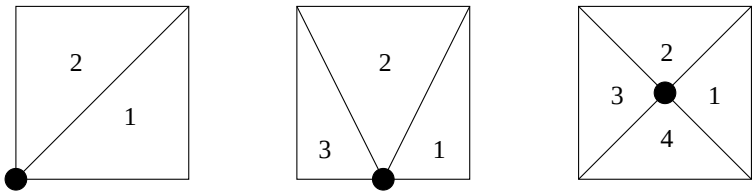


(a) Collocation at $\boldsymbol{\eta} = (-1, -1)$.

(b) Collocation at $\boldsymbol{\eta} = (0, -1)$.

(c) Collocation at $\boldsymbol{\eta} = (0, 0)$.

**Figure 4.2:** Element subdivision into triangles, for different collocation points.

As long as the boundary element is non-degenerate (i.e. the mapping from the parent to the phsyical element one-to-one) it further follows that the function $\hat{r}(\rho, \alpha; \boldsymbol{\eta})$ is nonzero for $\rho = 0$, where $\hat{r}$ is defined by the equation:

$$r = |\boldsymbol{x} - \boldsymbol{y}_{n_c}| = \rho \left| \sum_{q=1}^{9} \hat{\phi}_q(\rho, \alpha; \boldsymbol{\eta}) \boldsymbol{x}^{m(e,q)} \right| = \rho \hat{r}(\rho, \alpha; \boldsymbol{\eta}).$$

Using the polar coordinates and the function $\hat{r}$, the Green's tensor can be rewritten as:

$$\Sigma_{ij}^k(\boldsymbol{x}^e(\boldsymbol{\xi}), \boldsymbol{y}_{n_c}) = \frac{1}{\rho^2} \hat{\Sigma}_{ij}^k(\rho, \alpha; \boldsymbol{\eta}),$$

where $\hat{\Sigma}_{ij}^k$ is nonsingular for $\rho = 0$. With $\mathrm{d}\xi_1 \mathrm{d}\xi_2 = \rho \, \mathrm{d}\rho \mathrm{d}\alpha$ it now follows that the integral (4.3c) may be rewritten as:

$$\begin{aligned} &\int_{E_e} [u_i(\boldsymbol{x}) - u_i(\boldsymbol{y}_{n_c})] \Sigma_{ij}^k(\boldsymbol{x}, \boldsymbol{y}_{n_c}) \mathrm{n}_j(\boldsymbol{x}) \, \mathrm{d}S_{\boldsymbol{x}} \\ &\qquad = \int_{\alpha_1}^{\alpha_2} \int_{\rho_1(\alpha)}^{\rho_2(\alpha)} \sum_{q=1}^{9} \rho \hat{\phi}_q(\rho, \alpha; \boldsymbol{\eta}) u_i^{m(e,q)} \frac{1}{\rho^2} \hat{\Sigma}_{ij}^k(\rho, \alpha; \boldsymbol{\eta}) \mathrm{n}_j^e(\rho, \alpha; \boldsymbol{\eta}) \rho \, \mathrm{d}\rho \mathrm{d}\alpha, \quad (4.4) \end{aligned}$$

such that the singular factor $1/\rho^2$ is cancelled and the resulting integral nonsingular.

For the numerical integration it remains to determine the limits $(\alpha_1, \alpha_2)$ and $(\rho_1(\alpha), \rho_2(\alpha))$ and transform the integral (4.4) to rectangular coordinates, such that ordinary Gauss quadrature can be used. This is achieved by first performing the parent element subdivision into triangles of Rezayat et al. [51], illustrated in Fig. 4.2. Figure 4.2(a) shows the subdivision into two triangles for the case of corner node collocation, in the depicted case at node $q = 1$. Figure 4.2(b) shows the subdivision into three triangles for the case of midside node collocation, in the figure illustrated with collocation at node $q = 2$. For the collocation at the centre node, $q = 9$, in Fig. 4.2(c) a subdivision into four triangles is used as illustrated. For each triangle the four parameters $\{\alpha_1, \alpha_m, \alpha_2, \rho_0\}$ depicted in Fig. 4.3 are introduced, such that each triangle is defined by $(\rho, \alpha) \in [0, \rho_0 / \cos(\alpha - \alpha_m)] \times [\alpha_1, \alpha_2]$.

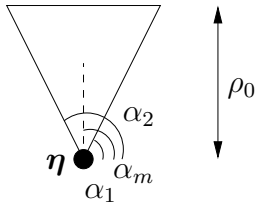


**Figure 4.3:** The four parameters introduced to define the subdivision triangles.

Here $\alpha_m = 0, \pi/2, \pi$ or $3\pi/2$ and $\rho_0 = 1$ or 2, depending on the triangle. The final transformation to rectangular coordinates is performed by introducing the substitution of variables $(v_1, v_2) \in [-1, 1] \times [-1, 1] \rightarrow (\rho, \alpha)$ defined by:

$$\begin{cases} \rho = \dfrac{\rho_0}{2\cos(\alpha - \alpha_m)}(1 + v_1), \\ \alpha = \dfrac{\alpha_2 - \alpha_1}{2} v_2 + \dfrac{\alpha_2 + \alpha_1}{2}. \end{cases}$$

In conclusion, by using indirect regularization in combination with an isoparametrical interpolation with Lagrangian interpolation functions, modified interpolation functions, element subdivision and a final transformation to rectangular coordinates, the singular element integrals are transformed to regular integrals which can be accurately computed using ordinary Gauss quadrature.

## 4.2 Truncation of infinite boundaries

In applications of the boundary element method to unbounded boundaries, such as the back surfaces in papers A-D, there are two main possible alternatives; 1): to truncate the boundary and restrict the discretization to a finite part of it, or 2): to use the knowledge of the asymptotic behaviour of the fields at infinity, for example through infinite boundary elements [6, 11, 24]. As discussed by Arias and Achenbach [6] and Domínguez and Meise [30], as long as the propagating waves exhibit attenuation the first alternative generally works well. This is the case in 3D elastodynamics, where all propagating waves normally exhibit geometrical attenuation. For the 2D P-SV case, on the other hand, the existence of Rayleigh surface waves propagating along the boundary without attenuation can lead to significant errors due to reflections from the ends of the truncated boundary element mesh. The use of infinite boundary elements is then a good alternative. If, on the other hand, material damping is included then all propagating waves exhibit attenuation such that simply truncating the boundary at sufficient distances from the region of interest works well. In this thesis infinite elements are not employed, since for the 2D SH case in paper A the waves exhibit geometrical attenuation and in papers B-D material damping

is included.

# 5 Summaries of appended papers

**Paper A**, *2D SH modelling of ultrasonic testing for cracks near a non-planar surface.* The paper presents a 2D SH model of ultrasonic testing for interior cracks near a non-planar back surface in a thick-walled solid. The model is based on a novel solution method which reformulates the wave scattering problem as two coupled boundary integral equations (BIEs); a hypersingular traction BIE for the crack opening displacement (COD) and a regularized displacement BIE for the back surface displacement. The method then solves the integral equations simultaneously, after a discretization using a series expansion of the COD in Chebyshev functions and a boundary element discretization of the back surface displacement. The action of an ultrasonic contact probe in transmission is modelled by prescribing the traction on the surface beneath it, while an electromechanical reciprocity relation is used to model the action of the receiving ultrasonic probe.

**Paper B**, *A 2D model of ultrasonic testing for cracks near a non-planar surface.* An extension of the work in paper A is presented in this paper, treating the 2D P-SV case which features coupled compressional and shear wave motions. The wave scattering problem is solved using an extended version of the solution method developed in paper A, and the action of the receiving ultrasonic contact probe is modelled using the same reciprocity relation. Material damping is also included in the model. The transmitting ultrasonic probe is again modelled by prescribing the traction on the surface beneath it, but in order to model both P and SV probes two different tractions are considered. The influence of a couplant applied between the probe and the component to increase the transmission of energy is also accounted for in this probe model.

**Paper C**, *Elastic wave scattering by a rectangular crack near a non-planar back surface.* In this paper the solution methods of papers A and B are extended to 3D, for the case of elastic wave scattering by an interior rectangular crack in a thick-walled component with a back surface of general geometry. The solution method is used to form the basis of a 3D model of ultrasonic testing, which also takes into account material damping, the action of ultrasonic contact probes in transmission and reception, and calibration by a side-drilled hole. The solution method generates many unknowns and consequently leads to demanding computations, but by employing the stationary phase approximation for the computation of probe field integrals and a threshold criterion to generate a sparse approximation of the system matrix, the computations become viable.

**Paper D**, *A hybrid $T$ matrix/boundary element method for elastic wave scattering from defects near a non-planar surface.* A novel solution method based on a hybrid $T$ matrix/boundary element approach is developed in this paper. The approach uses a boundary integral equation for the non-planar surface, in which the scattering by the defect is accounted for by incorporating the transition ($T$) matrix of the defect in the Green's tensor

used in the integral equation. To solve the integral equation the boundary element method is used. By incorporating the solution method in the model framework of paper B, a model of ultrasonic testing for defects located near a non-planar surface is developed. Since it is possible to compute the $T$ matrix of any defect (e.g. by a direct numerical method), the model can in principle treat all defects. Most interesting for applications, however, are the defects for which fast, analytically oriented computations of the $T$ matrix are possible. An example of such defects is the circular cavity used in the numerical examples, for which the $T$ matrix can be very efficiently computed by separation-of-variables.

# 6 Concluding remarks and future work

In this thesis solution methods for elastic wave scattering by defects near non-planar surfaces are developed. The methods are based on frequency domain boundary integral equation methods, with a focus on analytical approaches for the defects and regularized boundary element methods for the back surfaces. This leads to efficient treatments of the defects which take into account possibly singular behaviour at defect edges, while the back surfaces are allowed to be of general, complex geometry. All hypersingular crack integrals are evaluated analytically, while numerical computation of singular boundary element integrals is avoided by employing indirect regularization techniques. Another characteristic feature of the solution methods is their ability to generate accurate results for both low, intermediate and high frequencies.

In order to develop measurement models of ultrasonic nondestructive testing, the solution methods are incorporated into a framework of transmitting probe models based on prescribing the traction underneath the probe and receiving probe models based on electromechanical reciprocity. It is also shown how calibration, effects of material damping and the computation of time traces can be incorporated.

For a strip-like crack in 2D, both the cases of anti-plane and in-plane wave propagation are treated. The work is also extended to the 3D case with a rectangular crack. In an effort to treat more general defect types, a solution method based on the $T$ matrix representation of defects is also developed. This is done for the 2D in-plane wave propagation, but the method could readily be extended to 3D. The computations would become rather demanding and time-consuming, but with the developments of increasing computational power this issue should be of minor importance within a perspective of a few years.

For the practical value of the models, common test object geometries should be identified and parametrised such that they can be easily simulated using the models. A useful extension of the work would be to also include models of phased arrays and focused ultrasonic probes.

Numerical results are presented in the papers such that comparisons with, and verifications against, other models can be made. Even more important for ultrasonic measurement models, however, is experimental validation. Participation in benchmark studies, for ex-

ample at the Annual Review of Progress in Quantitative Nondestructive Evaluation [47], to validate the models is thus a recommended course of future work.

# References


[1] J.D. Achenbach. *Wave Propagation in Elastic Solids*. North-Holland, Amsterdam, 1973.

[2] J.D. Achenbach. Measurement models for quantitative ultrasonics. *J. Sound Vib.*, 159:385–401, 1992.

[3] J.D. Achenbach. Quantitative nondestructive evaluation. *Int. J. Solids Struct.*, 37:13–27, 2000.

[4] J.D. Achenbach. Modeling for quantitative non-destructive evaluation. *Ultrasonics*, 40:1–10, 2002.

[5] J.D. Achenbach and A.K. Gautesen. Geometrical theory of diffraction for three-D elastodynamics. *J. Acoust. Soc. Am.*, 61:413–421, 1977.

[6] I. Arias and J.D. Achenbach. Rayleigh wave correction for the BEM analysis of two-dimensional elastodynamic problems in a half-space. *Int. J. Numer. Meth. Engng.*, 60:2131–2146, 2004.

[7] M.P. Ariza, A. Sáez, and J. Domínguez. A singular element for three-dimensional fracture mechanics analysis. *Eng. Anal. Boundary Elem.*, 20:275–285, 1997.

[8] ASNT - The American Society for Nondestructive Testing. Introduction to Nondestructive Testing, January 2011. `http://www.asnt.org/ndt/primer1.htm`.

[9] A. Bedford and D.S. Drumheller. *Introduction to Elastic Wave Propagation*. John Wiley & Sons, Chichester, 1994.

[10] G. Beer. *Programming the Boundary Element Method*. John Wiley & Sons Ltd, Chichester, 2001.

[11] P. Bettess. *Infinite elements*. Penshaw Press, Cleadon, 1992.

[12] J.P. Bingham and M.K. Hinders. Automatic multimode guided wave feature extraction using wavelet fingerprints. In Thompson and Chimenti [59].

[13] J. Blitz and G. Simpson. *Ultrasonic Methods of Non-destructive Testing*. Chapman & Hall, London, 1996.

[14] M. Bonnet. *Boundary Integral Equation Methods for Solids and Fluids*. John Wiley & Sons Ltd, Chichester, 1995.

[15] A. Boström. Multiple scattering of elastic waves by bounded obstacles. *J. Acoust. Soc. Am.*, 67:399–413, 1980.

[16] A. Boström. Acoustic scattering by a sound-hard rectangle. *J. Acoust. Soc. Am.*, 99:3344–3347, 1991.

[17] A. Boström. Review of hypersingular integral equation method for crack scattering and application to modeling of ultrasonic non-destructive evaluation. *Appl. Mech. Rev.*, 56:383–405, 2003.

[18] A. Boström and A.S. Eriksson. Scattering by two penny-shaped cracks with spring boundary conditions. *Proc. R. Soc. London A*, 443:183–201, 1993.

[19] A. Boström, T. Grahn, and A.J. Niklasson. Scattering of elastic waves by a rectangular crack in an anisotropic half-space. *Wave Motion*, 38:91–107, 2003.

[20] A. Boström and H. Wirdelius. Ultrasonic probe modeling and nondestructive crack detection. *J. Acoust. Soc. Am.*, 97:2836–2848, 1995.

[21] C.A. Brebbia. *The boundary element method for engineers*. Pentech Press, London, 1978.

[22] C.A. Brebbia and J. Dominguez. *Boundary Elements - An introductory course*. Computational Mechanics Publications, Southampton, 1989.

[23] C.A. Brebbia, J.C.F. Telles, and L.C. Wrobel. *Boundary element techniques : theory and applications in engineering*. Springer, Berlin, 1983.

[24] S. Bu. Infinite boundary elements for the dynamic analysis of machine foundations. *Int. J. Numer. Meth. Engng.*, 40:3901–3917, 1997.

[25] P. Bövik and A. Boström. A model of ultrasonic nondestructive testing for internal and subsurface cracks. *J. Acoust. Soc. Am.*, 102:2723–2733, 1997.

[26] P. Calmon, A. Lhémery, I. Lecœur-Taïbi, R. Raillon, and L. Paradis. Models for the computation of ultrasonic fields and their interaction with defects in realistic NDT configurations. *Nucl. Eng. Des.*, 180:271–283, 1998.

[27] CEA - The French Atomic Energy Commission. CIVA: State of the art simulation software for Non Destructive Testing, January 2011. `http://www-civa.cea.fr`.

[28] R.K. Chapman. A system model for the ultrasonic inspection of smooth planar cracks. *J. Nondestr. Eval.*, 9:197–210, 1990.

[29] A.H.-D. Cheng and D.T. Cheng. Heritage and early history of the boundary element method. *Eng. Anal. Boundary Elem.*, 29:268–302, 2005.

[30] J. Dominguez and T. Meise. On the use of the BEM for wave propagation in infinite domains. *Eng. Anal. Boundary Elem.*, 8:132–138, 1991.

[31] J. Domínguez. *Boundary Elements in Dynamics*. Computational Mechanics Publications, Southampton, 1993.

[32] D. Ensminger. *Ultrasonics - Fundamentals, Technology, Applications*. Marcel Dekker, New York, 1988.

[33] P. Fellinger, R. Marklein, K.J. Langenberg, and S. Klaholz. Numerical modeling of elastic wave propagation and scattering with EFIT-elastodynamic finite integration technique. *Wave Motion*, 21:47–66, 1995.

[34] L. Guan and A. Norris. Elastic wave scattering by rectangular cracks. *Int. J. Solids Struct.*, 29:1549–1565, 1992.

[35] S. Halkjær. *Elastic wave propagation in anisotropic, inhomogeneous materials - application to ultrasonic NDT*. PhD thesis, Technical University of Denmark, Lyngby, 1999.

[36] M.K. Hinders and J.P. Bingham. Lamb wave pipe coating disbond detection using the dynamic wavelet fingerprinting technique. In Thompson and Chimenti [59].

[37] P. Huthwaite, F. Simonetti, and M.J.S. Lowe. On the convergence of finite element scattering simulations. In Thompson and Chimenti [59].

[38] J. B. Keller. Geometrical theory of diffraction. *J. Opt. Soc. Am.*, 52:116–130, 1962.

[39] E.A. Kraut. Review of Theories of Scattering of Elastic Waves by Cracks. *IEEE Trans. Sonics and Ultrasonics*, SU-23:162–167, 1976.

[40] J. Krautkrämer and H. Krautkrämer. *Ultrasonic Testing of Materials*. Springer, Berlin, 1990.

[41] H. Kuttruff. *Ultrasonics - fundamentals and applications*. Elsevier Applied Science, London, 1991.

[42] S. Lin, H. Yamada, H. Fukutomi, and T. Ogata. Prediction of received signals in ultrasonic testing by finite element method combined with geometrical optics theory. In Thompson and Chimenti [58].

[43] Y. Liu and F.J. Rizzo. Scattering of elastic waves from thin shapes in three dimensions using the composite boundary integral equation formulation. *J. Acoust. Soc. Am.*, 102:926–932, 1997.

[44] P. McIntire, editor. *Nondestructive Testing Handbook*, volume 7. The American Society for Nondestructive Testing, 1991.

[45] N. Nishimura and S. Kobayashi. A regularized boundary integral equation method for elastodynamic crack problems. *Comp. Mech.*, 4:319–328, 1989.

[46] Y-H. Pao. Betti's identity and transition matrix for elastic waves. *J. Acoust. Soc. Am.*, 64:302–310, 1978.

[47] QNDE Programs. QNDE - Review of Progress in Quantitative Nondestructive Evaluation, February 2011. `http://www.qndeprograms.org/`.

[48] R. Raillon, S. Bey, A. Dubois, S. Mahaut, and M. Darmon. Results of the 2009 UT modeling benchmark obtained with CIVA: Responses of notches, side-drilled holes and flat-bottom holes of various sizes. In Thompson and Chimenti [59].

[49] R. Raillon, S. Mahaut, N. Leymarie, and M. Spies. Results of the 2008 UT modeling benchmark obtained with 2 semi-analytical models: Responses of flat bottom holes at various depths under interfaces of different curvatures. In Thompson and Chimenti [58].

[50] P. Rajagopal, M. Drozdz, and M.J.S. Lowe. Towards improved finite element modeling of interaction of elastic waves with complex defect geometries. In Thompson and Chimenti [58].

[51] M. Rezayat, D.J. Shippy, and F.J. Rizzo. On time-harmonic elastic-wave analysis by the boundary element method for moderate to high frequencies. *Comp. Meth. Appl. Mech. Engng.*, 55:349–367, 1986.

[52] L.W. Schmerr. *Fundamentals of Ultrasonic Nondestructive Evaluation*. Plenum Press, New York, 1998.

[53] A. Sáez and J. Domínguez. BEM analysis of wave scattering in transversely isotropic solids. *Int. J. Numer. Meth. Engng.*, 44:1283–1300, 1999.

[54] A. Sáez, R. Gallego, and J. Domínguez. Hypersingular quarter-point boundary elements for crack problems. *Int. J. Numer. Meth. Engng*, 38:1681–1701, 1995.

[55] M.G. Silk. *Ultrasonic Transducers for Nondestructive Testing*. Adam Hilger, Bristol, 1984.

[56] V. Sladek and J. Sladek, editors. *Singular Integrals in Boundary Element Methods*. Advances in Boundary Element Series. Computational Mechanics Publications, Southampton, 1998.

[57] I.S. Sokolnikoff. *Mathematical Theory of Elasticity*. McGraw-Hill, New York, 1956.

[58] D.O. Thompson and D.E. Chimenti, editors. *Review of Progress in Quantitative Nondestructive Evaluation*, volume 28. American Insitute of Physics, New York, 2009.

[59] D.O. Thompson and D.E. Chimenti, editors. *Review of Progress in Quantitative Nondestructive Evaluation*, volume 29. American Insitute of Physics, New York, 2010.

[60] R.B. Thompson and T.A. Gray. Use of ultrasonic models in the design and validation of new NDE techniques. *Proc. R. Soc. London A*, 320:329–340, 1986.

[61] V.V. Varadan, A. Lakhtakia, and V.K. Varadan, editors. *Field Representations and Introduction to Scattering*, volume 1 of *Acoustic, electromagnetic and elastic wave scattering*. North-Holland, Amsterdam, 1991.

[62] A. Velichko and P.D. Wilcox. Efficient finite element modelling of elastodynamic scattering. In Thompson and Chimenti [59].

[63] P.C. Waterman. Matrix theory of elastic wave scattering. *J. Acoust. Soc. Am.*, 60:567–580, 1976.

[64] H. Wirdelius. *Ultrasonic NDT in Defect Detection - Mathematical Modelling.* PhD thesis, Chalmers University of Technology, Göteborg, 1995.

[65] Ch. Zhang and D. Gross. *On Wave Propagation in Elastic Solids with Cracks.* Computational Mechanics Publications, Southampton, 1998.